Journal of Translational Medicine

RESEARCH

Open Access

Revealing multiple biological subtypes of schizophrenia through a data-driven approach

Yuran Wang[1], Shixuan Feng[2], Yuanyuan Huang[2,4], Runlin Peng[1], Liqin Liang[1], Wei Wang[1], Minxin Guo[1], Baoyuan Zhu[1], Heng Zhang[1], Jianhao Liao[1], Jing Zhou[3,4,5,6], Hehua Li[2,4], Xiaobo Li[8], Yuping Ning[2,4], Fengchun Wu[2,4,9*] and Kai Wu[1,7,10*]

Abstract

Introduction The brain imaging subtypes of schizophrenia have been widely investigated using data-driven approaches. However, the heterogeneity of SZ in multiple biological data is largely unknown.

Methods A data-driven model was used to classify brain imaging, gut microbiota, and brain-gut fusion data obtained through a dot product fusion method, identifying significant subtypes and calculating their correlations with clinical symptoms and cognitive performance.

Results These subtypes remain relatively independent and demonstrate typical features and biomarkers, which are significantly associated with clinical symptoms and cognitive performance. Two brain subtypes with opposite structural and functional changes are identified: (1) a structural variant-dominant brain subtype with negative symptoms and cognitive deficits and (2) a functional alteration-dominant brain subtype with positive symptoms. The three gut subtypes include the following: (1) *Collinsella*-dominant; (2) *Prevotella*-dominant with positive symptoms; and (3) *Streptococcus*-dominant. Two brain-gut subtypes show different abnormalities in brain–genus linkages: (1) strong connectivity of "brain function in the temporal and parietal lobes–*Prevotella*" with reduced attention scores and (2) strong connectivity of "brain structure and function in the frontal and parietal lobes–multiple genera" with positive symptoms. Notably, brain subtypes and brain-gut subtypes are most relevant to clinical symptoms, whereas gut subtypes reveal more cognitive biomarkers.

Conclusion These findings show the potential to identify multiple biological subtypes with distinct biomarkers, thereby suggesting the possibility of personalized and precise treatment for SZ patients.

Keywords Brain imaging, Gut microbiota, Brain-gut axis, Data-driven, Schizophrenia, Subtypes, Biomarkers

*Correspondence:
Fengchun Wu
2018760372@gzhmu.edu.cn
Kai Wu
kaiwu@scut.edu.cn

Full list of author information is available at the end of the article

Introduction

Schizophrenia (SZ) is a severe psychiatric disorder characterized by various complex symptoms, including delusions, hallucinations, emotional apathy and social withdrawal [1–3]. While the current evidence has established schizophrenia as a multifactorial disorder involving aberrant neurodevelopmental, neurochemical, and neuroimmune pathways, the exact pathogenic mechanisms remain elusive [4, 5]. The traditional diagnostic assessment of SZ is mainly based on clinical interviews and scales measuring clinical symptoms [6]. However, previous research on SZ has revealed substantial heterogeneity in terms of clinical symptoms, treatment and biological markers [7–10]. Due to heterogeneity, the treatment response in patients with SZ varies, suggesting the existence of different subtypes caused by their internal biological mechanisms [9, 10]. Identifying various subtypes using biological data could help to overcome the challenges stemming from heterogeneity [11].

Over the past two decades, rapid advancements in brain imaging methods, including structural magnetic resonance imaging (sMRI) and resting-state functional magnetic resonance imaging (rs-fMRI), have provided clinicians with an unparalleled opportunity to noninvasively explore brain structure and function in SZ patients [12, 13], and have offered valuable insights into its neurobiological mechanisms and molecular biomarkers [14, 15]. Importantly, a number of data-driven neuroimaging studies have considerably expanded methodological theories and applied research in brain subtypes of SZ, leading to novel achievements and breakthroughs in understanding the heterogeneity of SZ in patients. The alterations in brain structure in patients with different SZ subtypes vary, affecting both cortical and subcortical regions, with widespread alterations in white matter volume (WMV) also observed across different subtypes [16, 17]. Functional connectivity (FC) exhibit variability across multiple brain regions between patients with different SZ subtypes, particularly in the lateral frontal cortex, temporoparietal junction, precuneus, and anterior temporal lobe network [18, 19]. Additionally, clinical symptoms and cognitive performance are significantly different between patients with different SZ subtypes. Recent studies revealed that salience network-centered hypoconnectivity is correlated with severe clinical symptoms and attention deficits, whereas the other subtypes are characterized by hyperconnectivity with greater cognitive flexibility impairments, and patients with the different subtypes demonstrate different symptom progression trajectories over time [11, 20]. These findings are critical for understanding the heterogeneity of SZ patients; however, most of them are inconsistent and cannot be validated across studies. These differences might be due to several factors, including early neurodevelopment during childhood and adolescence and the duration and treatment of the disease [21–23].

Recently, a large amount of evidence has indicated that the gut microbiota may play a crucial role in the pathophysiology of SZ in patients [24]. Although the abundance of the gut microbiota, such as *Veillonella* and *Bilophila*, in SZ patients has shown consistent trends across several studies [25–28], significant heterogeneity in the abundance of the gut microbiota has been observed in many other studies [29]. Specifically, some studies have reported conflicting findings on *Blautia* abundance, with one reporting a reduction in SZ patients compared with healthy controls (HCs) and the other reporting an increase [28, 30]. These discrepancies may be attributable to variations in the sample size or the influence of antipsychotic medication. Similarly, findings on *Enterococcus* also vary. A study involving 40 first-episode SZ patients, 85 chronically antipsychotic-treated SZ patients, and 69 HCs reported that *Enterococcus* levels were elevated in chronically treated SZ patients compared with HCs [25]. This finding is associated with antipsychotic treatment-related alterations in the gut microbiota, suggesting that prolonged antipsychotic use may significantly impact the gut microbial composition. However, another study revealed that *Enterococcus* levels were reduced in SZ patients [24]. Additionally, mixed results have been reported for *Lactobacillus*, as it was enriched in SZ patients in one study but significantly decreased in another; it is also noted for its potential probiotic benefits, particularly in weight management and metabolic conditions such as obesity and diabetes [30, 31]. Furthermore, recent studies reported that SZ patients with deficits had high levels of *Mycobacterium avium* and cognitive impairments, whereas SZ patients without deficits had even higher *M. avium* levels but were less prone to cardiovascular disease [32, 33]. Although numerous studies have revealed alterations in the gut microbiota of SZ patients, the lack of definitive conclusions may stem from an oversight of the intrinsic subtypes of the disorder. The absence of individualized analyses has also hindered the identification of consistent gut microbial markers, which likely contributes to the seemingly contradictory findings across these studies [34].

The brain–gut axis is a bidirectional communication pathway between the central and enteric neural systems that has long been recognized for maintaining homeostasis [35, 36]. Recent advances have demonstrated that the gut microbiota influences the brain through diverse metabolic and immunological pathways, with studies on the brain–gut axis in SZ patients further revealing its significant role in modulating the pathophysiology and clinical symptoms of this disorder [37–39]. Specific stool bacteria can trigger SZ-like behavioral changes by reducing glutamate levels and increasing glutamate, glutamine,

and gamma-aminobutyric acid concentrations in the hippocampus [37]. Specifically, *Sellimonas* and *Roseburia* play crucial roles in the brain–gut axis, with *Sellimonas* being positively correlated with negative symptoms in SZ patients and potentially influencing brain network properties, whereas *Roseburia* is associated with gut health and immune regulation, making these microbes promising biomarkers for the severity of SZ symptoms [40, 41]. In addition, probiotics such as *Lactobacillus* and *Bifidobacterium* have been shown to increase the antioxidant capacity in vivo and reduce pathogenic inflammation via their effects on metabolic pathways [38]. Furthermore, particular bacteria influence brain development and neuroplasticity by altering neurotrophic factors, including brain-derived neurotrophic factor, and N-methyl-D-aspartate receptors [39]. These studies have shown the great potential of the brain–gut axis for exploring the pathology of SZ. Despite these advances, few systematic studies have further addressed the heterogeneity of the brain–gut axis in SZ patients [42].

In this study [43], we applied a data-driven approach to systematically investigate three subtypes of SZ using brain imaging data (SZ = 250, HCs = 300), gut microbiota data (SZ = 193, HCs = 123), and a fusion of brain–gut data (SZ = 43, HCs = 55). We analyzed distinct features between subtypes and explored correlations between these features and the scales of clinical symptoms and cognitive performance of patients with each subtype. Moreover, we aimed to determine the overlap between the multiple biological SZ subtypes.

Materials and methods

Participants

Participants in this study were recruited from 768 individuals (SZ = 400, HCs = 368) at the Affiliated Brain Hospital of Guangzhou Medical University and the Center for Biomedical Studies Excellence (COBRE) dataset, matched for sex, age, education, and lower body mass index (BMI). We recruited 633 Chinese Han participants (SZ = 333, HCs = 300) aged 18–60. The local brain dataset included sMRI and rs-fMRI data from 183 SZ patients and 232 HCs, while stool samples were collected from 193 SZ patients and 123 HCs. The two datasets overlapped in 98 participants (SZ = 43, HCs = 55). The brain subtypes (BSs) were studied using the local brain dataset as the training dataset and COBRE as the validation dataset. For the gut subtypes (GSs) and brain–gut subtypes (B-GSs), 80% of the dataset was randomly screened to be used as the training dataset, and the rest was used as the validation dataset. The scores for the first five dimensions of the Positive and Negative Symptom Scale (PANSS) and the MATRICS Consensus Cognitive Battery (MCCB) scales were collected for all participants. Table 1 provides a summary of the participants' demographic information, with averages used for missing data.

The diagnosis of SZ was based on DSM-IV-TR criteria, with patients diagnosed by clinical psychiatrists and having a disease duration of > 2 years. The specific exclusion criteria are described in Supplemental Method S1. The study followed the Declaration of Helsinki [44], and was approved by the Ethics Committee of the Affiliated Brain Hospital, Guangzhou Medical University (approval No. (2019)016). Informed consent was obtained from all participants or their legal guardians.

MRI data preprocessing and brain feature extraction

All MR images for the local brain dataset were acquired using a 3.0-T Philips MR scanner (Philips, Achieva, the Netherlands) at the Affiliated Brain Hospital, Guangzhou Medical University. Participants were instructed to rest quietly, breathe steadily, close their eyes, and minimize movement during the scan. T1-weighted sMRI images were obtained using the MPRAGE sequence and rs-fMRI images were collected using the EPI sequence. The MRI acquisition parameters are described in Supplemental Method S2. MRI images from different sites were calibrated in multiple centers. Images of all enrolled participants had no excessive head movements (head translation < 3 mm or rotational movement less than 3°).

The preprocessing steps for both sMRI and rs-fMRI were conducted using SPM8 and DPABI [45]. This part is the same as our previous multi-experiment [46–48, 49], as described in Supplemental Method S3. In brief, we use the gray matter volume (GMV), white matter volume (WMV), amplitude of low-frequency fluctuation (ALFF) and regional homogeneity (ReHo), FC matrix and the network features (clustering coefficient and global efficiency). Additionally, this study employed the AAL template and eight brain networks: the default mode network (DMN), the somatomotor network (SMN), the visual network (VSN), the dorsal attentional network (DAN), the ventral attentional network (VAN), the frontoparietal network (FPN), the subcortical network (SCN), and the limbic network (LN) [50–54].

Stool sample collection and gut feature extraction

Stool sample collection and gut feature extraction methods were similar to those described in our previous studies [40, 41, 55, 56], and the specific methodology as in the Supplemental Methods S4. In this study, we removed 176 genera that were missing in more than 10% of the participants. Finally, we selected *Collinsella*, *Faecalibacterium*, *Clostridium*, *Blautia*, *Gemmiger*, *Bacteroides*, *Prevotella*, *Lachnospira*, *Roseburia*, *Bifidobacterium*, *Bilophila*, *Dorea*, *Oscillospira*, *Streptococcus*, *Anaerostipes*, *Parabacteroides*, *Phascolarctobacterium*, *Coprococcus*, *Ruminococcus*, and *Veillonella* as the core genera for human

Table 1 Demographic information of SZ patients and HCs from each site. a)

a)						
Institution	**Brain local dataset (*n* = 415)**			**Brain COBRE (*n* = 135)**		
Group	SZ (*n* = 183)	HCs (*n* = 232)	$p_{Bonferroni}$	SZ (*n* = 67)	HCs (*n* = 68)	$p_{Bonferroni}$
Sex (female/male)	65/118	91/141	1	13/54	23/45	0.531
Age (years)	34.22 ± 0.66	33.25 ± 0.60	1	37.82 ± 1.69	35.98 ± 1.43	1
Education (years)	11.43 ± 0.22	11.14 ± 0.18	1	12.90 ± 0.24	11.71 ± 0.40	0.189
BMI (kg/m²)	23.51 ± 0.23	23.04 ± 0.21	1	——	——	——
PANSS PScore	20.29 ± 0.54	——	——	14.75 ± 0.58	——	——
PANSS NScore	21.59 ± 0.56	——	——	14.45 ± 0.59	——	——
PANSS GScore	38.18 ± 0.74	——	——	29.06 ± 1.04	——	——
PANSS TScore	80.06 ± 1.54	——	——	58.25 ± 1.71	——	——
Processing Speed	33.35 ± 1.51	47.85 ± 0.61	< 0.001	36.03 ± 1.49	53.51 ± 1.10	< 0.001
Attention/Vigilance	37.08 ± 1.06	49.17 ± 0.60	< 0.001	37.11 ± 1.76	49.13 ± 1.08	< 0.001
Working Memory	36.89 ± 1.35	43.65 ± 0.68	< 0.001	39.90 ± 1.59	50.30 ± 1.35	< 0.001
Verbal Learning	35.69 ± 1.55	47.22 ± 0.63	< 0.001	38.47 ± 1.04	46.57 ± 1.14	< 0.001
Visual Learning	39.11 ± 1.37	47.88 ± 0.62	< 0.001	36.84 ± 1.50	46.10 ± 1.29	< 0.001
First 5 d MCCB Score	182.40 ± 5.26	235.79 ± 2.09	< 0.001	188.35 ± 5.59	245.61 ± 3.95	< 0.001
b)						
Institution	**Gut local dataset (*n* = 316)**			**Brain–gut local dataset (*n* = 98)**		
Group	SZ (*n* = 193)	HCs (*n* = 123)	$p_{Bonferroni}$	SZ (*n* = 43)	HCs (*n* = 55)	$p_{Bonferroni}$
Sex (female/male)	82/111	59/64	1	20/23	24/31	1
Age (years)	42.98 ± 0.96	42.63 ± 1.17	1	34.26 ± 1.68	33.98 ± 1.37	1
Education (years)	11.18 ± 0.13	10.88 ± 0.11	1	12.30 ± 0.55	15.69 ± 0.40	0.010
BMI (kg/m²)	23.51 ± 0.19	23.27 ± 0.26	1	23.76 ± 0.65	22.18 ± 0.39	0.300
PANSS PScore	11.24 ± 0.32	——	——	11.00 ± 0.72	——	——
PANSS NScore	16.89 ± 0.47	——	——	18.53 ± 1.12	——	——
PANSS GScore	27.99 ± 0.46	——	——	32.65 ± 1.42	——	——
PANSS TScore	56.12 ± 0.98	——	——	62.19 ± 2.67	——	——
Processing Speed	33.25 ± 1.08	50.93 ± 0.82	< 0.001	36.58 ± 2.23	47.95 ± 1.14	< 0.001
Attention/Vigilance	36.49 ± 0.92	50.72 ± 0.82	< 0.001	38.84 ± 1.49	47.69 ± 1.20	< 0.001
Working Memory	36.72 ± 0.97	49.14 ± 0.78	< 0.001	39.47 ± 2.13	46.64 ± 1.10	0.050
Verbal Learning	33.74 ± 0.95	45.56 ± 0.88	< 0.001	34.58 ± 2.09	41.56 ± 1.18	0.040
Visual Learning	35.42 ± 1.04	48.22 ± 0.91	< 0.001	39.42 ± 2.09	46.69 ± 1.07	0.011
First 5 d MCCB Score	175.62 ± 3.92	244.57 ± 2.91	< 0.001	188.88 ± 7.98	230.53 ± 3.79	< 0.001

The data are reported as the means ± standard errors of the means. The PANSS PScore, PANSS NScore, PANSS GScore, and PANSS TScore represent the positive scores, negative scores, general cognitive scores, and total scores of the PANSS, respectively. Multiple comparisons are corrected by the Bonferroni correction

health before subsequent analysis [57]. The co-abundance network of the 20 selected genera was constructed using the SparCC technique, which calculates logarithmic scale variances to infer interrelationships among the genera [58]. Additionally, alpha diversity and relative abundance (RA) of these genera were extracted for further analysis.

Brain–gut feature fusion

To construct a brain–gut network and extract fusion features, we evaluated various fusion methods, with comparative results detailed in Supplemental Table S3. Building on these insights, we have developed a novel approach fusion method which called dot product fusion [59], wherein the brain feature matrix is transposed and element-wise multiplied with the gut feature matrix to capture interactions between corresponding brain and gut components. The mathematical formula for dot product fusion is as follows:

$$Z = X \circ Y^T \tag{1}$$

where ∘ denotes the Hadamard product (element-wise multiplication), Z is the fusion brain-gut feature matrix, X is the gut feature matrix, Y^T is the transpose of the brain feature matrix. Further methodological details and code are provided in Supplemental Method S5 and Supplemental Code S1.

Data-driven approach

A general linear model was used to remove the effects of covariates (sex, age, education, and BMI) before data input into the data-driven approach.

To address limitations of small-sample data and enhance classification accuracy, a denoising autoencoder (DAE) was employed for data enhancement. The DAE, comprising a noisy input, encoder, and decoder, was trained using the Adam optimizer, a batch size of 64, and 50 epochs, with the mean squared error as the loss function. Outputs from 10 cycles were averaged for robust results.

High-dimensional data from the DAE were reduced using independent component analysis (ICA) to extract key features. A hybrid clustering method combining k-means, Gaussian mixture model (GMM), and spectral clustering was applied, leveraging data similarity, probability density, and graph theory. This approach was chosen to integrate the strengths of different clustering techniques, ensuring robustness and adaptability for complex data structures compared to standard methods such as hierarchical clustering. Specific robustness comparisons are provided in Supplemental Table S1. The optimal number of clusters (2 to 15) was determined using the silhouette coefficient (SC) and Bayesian information criterion (BIC), while the adjusted rand index (ARI) was used to assess clustering reproducibility, with value closer to 1 indicating high reliability. Furthermore, as shown in Supplemental Table S2, sensitivity analyses were conducted using a controlled variable method on the brain imaging dataset to evaluate the impact of hyperparameter variations on clustering outcomes and subtype formation. These analyses informed our final selection of optimal hyperparameter settings for subtype formation.

Python (Ver.3.8) was used for all steps, including covariate removal, data enhancement, dimensionality reduction, clustering, and evaluation. The detailed workflow of methods is illustrated in Fig. 1. Detailed methodology can be found in Supplemental Methods S6.

Validation analysis and statistical analysis

The validation datasets underwent the same processes as the training datasets. A Kruskal–Wallis (KW) test with Bonferroni correction was used to compare subtype features between datasets. An adjusted $p_{Bonferroni} > 0.05$ indicated no significant differences, confirming subtype consistency.

Differences in BS, GS, and B-GS features were analyzed via KW tests with Bonferroni correction. Effect sizes were quantified by eta squared (η^2), and 95% confidence intervals (*CI*) were calculated for median difference. Adjusted $p_{Bonferroni} < 0.05$ indicating significant differences. Brain features, network connectivity, and genus relationships were compared between subtypes and HCs. Demographics, clinical symptoms, and cognitive performance were analyzed across subtypes. Pearson's correlation coefficients identified biomarkers (adjusted $p_{Bonferroni} < 0.05$) linked to PANSS and MCCB scores. Subtypes with sample sizes < 50 were resampled using the bootstrap method, averaging 1000 iterations [60].

We also performed mediation effect analyses to assess whether gut microbiota mediates the relationship between brain connectivity and cognitive function (brain-gut-scale) or whether brain connectivity mediates the relationship between gut microbiota and cognitive function (gut-brain-scale), using bootstrapped *CI* to evaluate indirect effects.

This section were conducted in Python (ver. 3.8). See more details in Supplemental Methods S7.

Results

Two brain subtypes with their corresponding biomarkers

Based on SC and BIC co-screening, two clusters were identified as the optimal number for BSs, with an ARI of 0.711, indicating high reproducibility. KW tests with Bonferroni correction confirmed that BS1 ($p_{Bonferroni}$ = 0.221) and BS2 ($p_{Bonferroni}$ = 0.335) from training and validation datasets could be considered the same subtypes. Detailed results and demographics are in Supplemental Figure S2 and Supplemental Table S4.

Compared to HCs, BS1 showed increased WMV in the frontal and temporal lobes, while BS2 had decreased WMV in the frontal lobe. Functionally, BS1 had increased ALFF and ReHo in the prefrontal and temporal lobes but decreased values in the occipital lobe, while BS2 showed the opposite pattern. Network features differed, with BS1 showing lower clustering coefficients ($\eta^2 = 0.253$, $p_{Bonferroni} < 0.001$, 95% *CI* = (0.001, 0.002)) and BS2 showing higher clustering coefficients ($\eta^2 = 0.210$, $p_{Bonferroni}$ = 0.022, 95% *CI* = (0.002, 0.006)) and global efficiency ($\eta^2 = 0.351$, $p_{Bonferroni}$ = 0.004, 95% *CI* = (-0.002, 0.000)).

Abnormal FC patterns also differed. BS1 had weak connectivity in SMN, VSN, LN, and DMN–SMN but stronger DMN and DMN-FPN connectivity. BS2 showed stronger occipital connectivity and weaker SMN, VAN, and DMN-LN connectivity. Clinical differences included higher PANSS positive ($\eta^2 = 0.219$, $p_{Bonferroni}$ = 0.004, 95% *CI* = (13.579, 15.913)) and total scores ($\eta^2 = 0.166$, $p_{Bonferroni}$ = 0.048, 95% *CI* = (54.833, 61.674)) for BS1, while MCCB scores differed significantly between BSs and HCs ($\eta^2 = 0.441$, $p_{Bonferroni} < 0.001$, 95% *CI* = (266.471, 302.863)).

Pearson's correlations revealed significant links between brain features and PANSS and MCCB scores, with WMV (BS1) and ALFF/ReHo (BS2) showing strong relationships. Notably, WMV in BS1 patients (r = -0.47, $p_{Bonferroni}$ = 7.78e-06), front area ALFF in BS2 patients (r = -0.60, $p_{Bonferroni}$ = 8.84e-12) and back area ReHo in BS2 patients ($r = 0.60$, $p_{Bonferroni}$ = 8.80e-12) were relevant to the PANSS scores. Additionally, the front area's ALFF for BS1 patients ($r = 0.40$, $p_{Bonferroni}$ = 8.32e-04) was highly

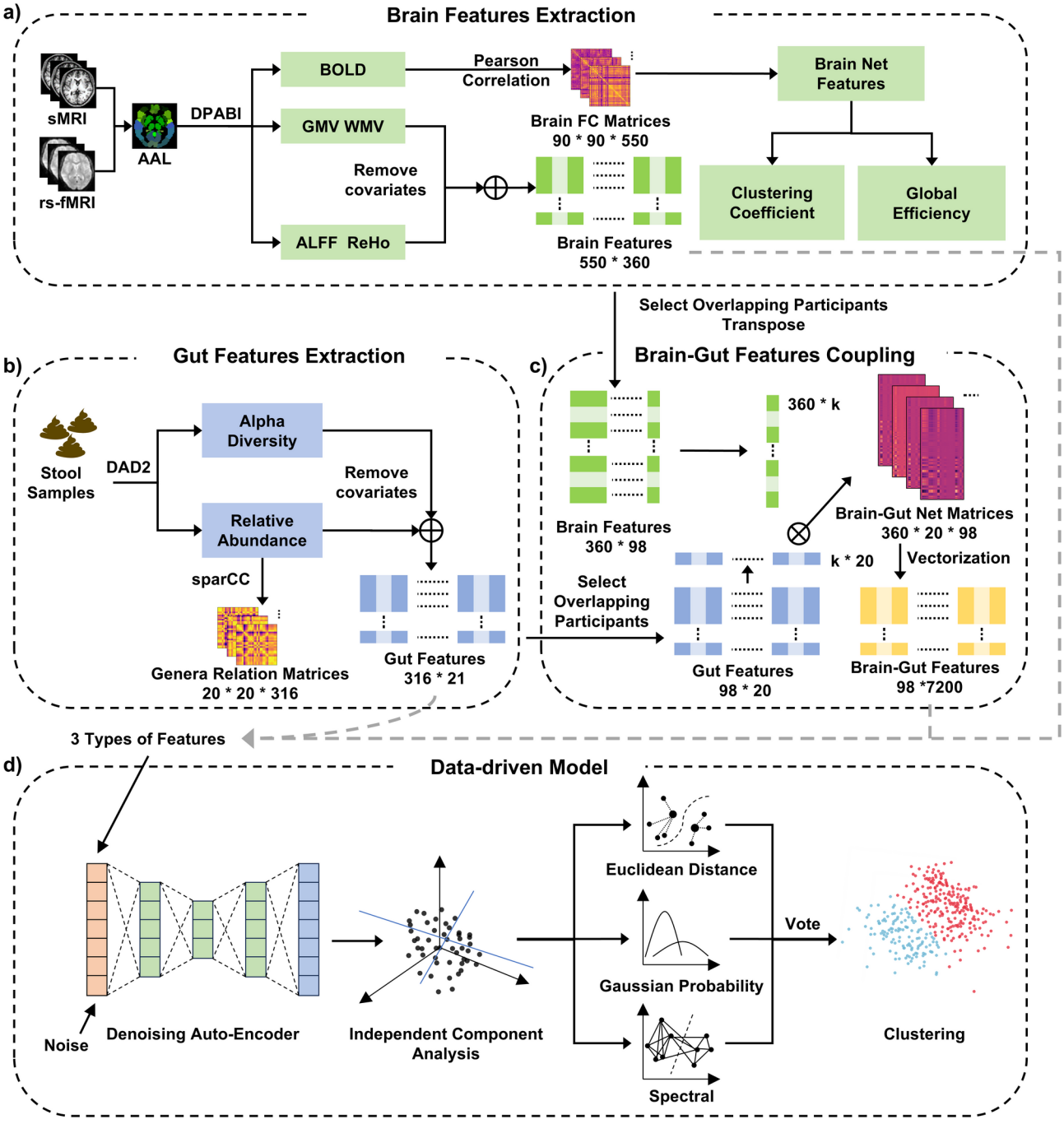

Fig. 1 The experimental methodology. (**a**) Method used to extract brain features. (**b**) Method used to extract gut features. (**c**) Method used for the fusion and extraction of brain–gut features. (**d**) Data-driven approach integrating the DAE for data enhancement, ICA for dimensionality reduction, k-means, GMM, and spectral methods for clustering

correlated with the MCCB scores. Key data are detailed in Fig. 2 and Supplemental Materials.

Three gut subtypes with their corresponding biomarkers

Based on SC and BIC analysis, three clusters were identified as the optimal GSs, with an ARI of 0.732, indicating high reproducibility. KW tests with Bonferroni correction confirmed consistency between training and validation datasets for GS1 ($p_{Bonferroni}$ = 0.965), GS2 ($p_{Bonferroni}$ = 0.131), and GS3 ($p_{Bonferroni}$ = 0.629). Detailed results and demographics are in Supplemental Figure S2 and Supplemental Table S6.

Alpha diversity differed significantly among GSs and HCs, with GS1 and GS3 showing higher diversity than

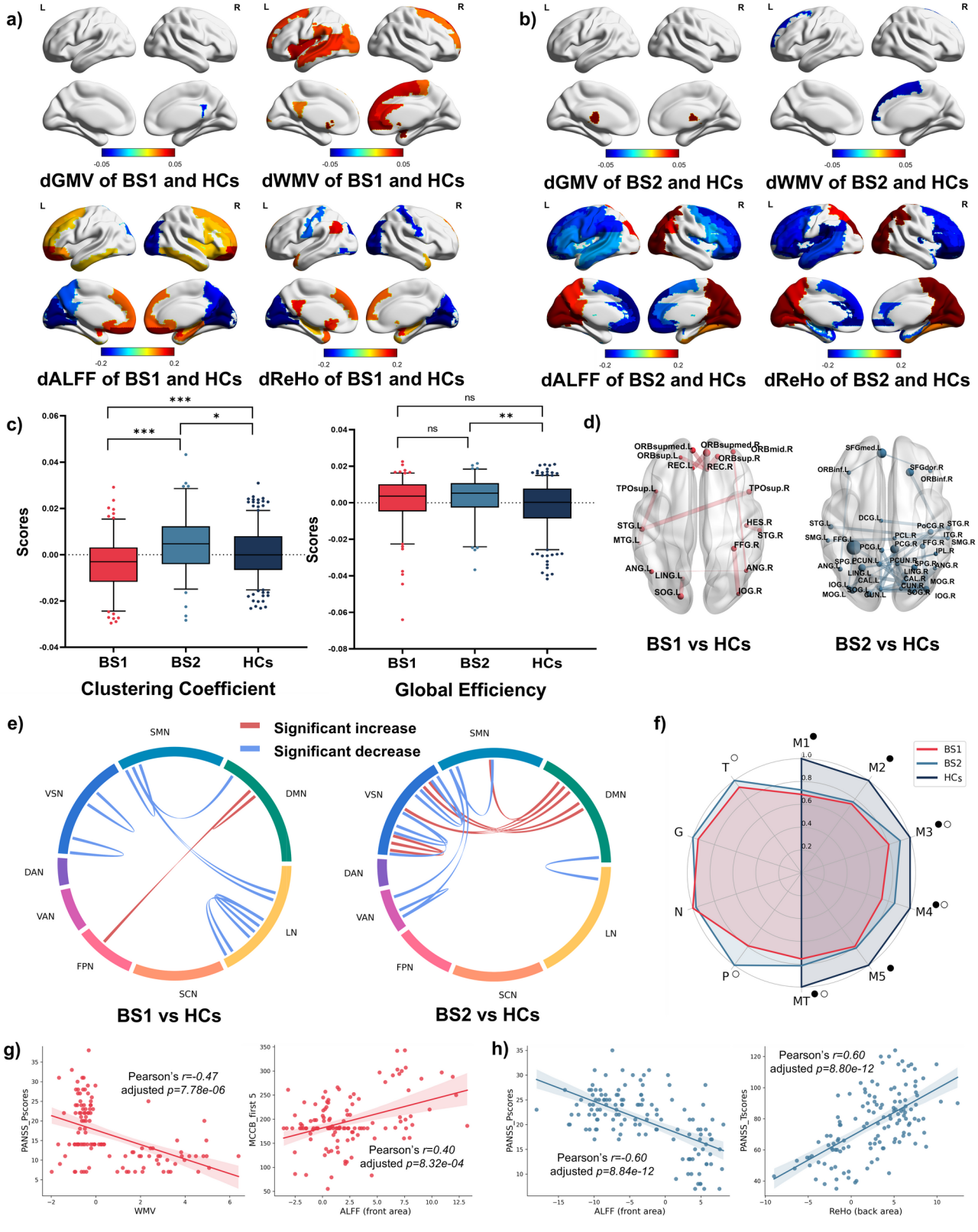

Fig. 2 (See legend on next page.)

(See figure on previous page.)

Fig. 2 Differences between the two brain subtypes and their corresponding biomarkers. (**a**) Comparison of differences in GMV, WMV, ALFF, and ReHo (dGMV, dGMV, dALFF, and dReHo) between BS1 patients and HCs. (**b**) Comparison of dGMV, dGMV, dALFF, and dReHo between BS2 patients and HCs. (**c**) Differences in the network features of the clustering coefficient and global efficiency between BSs and HCs. $^{*}p_{Bonferroni}< 0.05$, $^{**}p_{Bonferroni}< 0.01$, $^{***}p_{Bonferroni}< 0.001$. (**d**) Abnormal brain FC in BSs compared with HCs. (**e**) Brain FC abnormalities in BSs and the networks in which they reside are shown and compared with HCs. (**f**) Differences in clinical symptoms and cognitive performance between BSs and HCs (data are normalized), where P, N, G, and T represent PANSS PScore, NScore, GScore, TScore, respectively. M1-M5 and M represent processing speed, attention/vigilance, working memory, verbal learning, visual learning, and total scores of the first five dimensions of the MCCB, respectively. $^{\bullet}p_{all}< 0.05$ and $^{\circ}p_{BSs}< 0.05$ (with Bonferroni correction); all values are displayed in Supplemental Table S4. (**g**) Biomarkers of the PANSS and MCCB scores of BS1 patients. (**h**) Biomarkers of the PANSS scores of BS2 patients. The error bands in figures (**g**-**h**) represent 95% confidence interval

HCs (GS1: $\eta^2 = 0.291$, $p_{Bonferroni} < 0.001$, 95% *CI* = (5.739, 5.740); *GS3:* $\eta^2 = 0.347$, $p_{Bonferroni} < 0.001$, 95% *CI* = (5.736, 5.738)), while GS2 showed no significant difference. RA analysis revealed distinct genus profiles: GS1 had increased *Collinsella* ($\eta^2 = 0.222$, $p_{Bonferroni} = 0.003$, 95% *CI* = (-0.009, -0.004)), GS2 showed decreased *Gemmiger* ($\eta^2 = 0.553$, $p_{Bonferroni} = 0.037$, 95% *CI* = (-0.146, -0.010)) and increased *Prevotella* ($\eta^2 = 0.628$, $p_{Bonferroni} < 0.001$, 95% *CI* = (-0.020, -0.008)), and GS3 displayed a similar pattern to GS2 but with additional increases in *Streptococcus* ($\eta^2 = 0.305$, $p_{Bonferroni} = 0.033$, 95% *CI* = (0.000, 0.020)). These findings are in Fig. 3a-b and Supplemental Table S7.

Inter-genus relationships also varied. GS1 showed weaker connections than HCs, GS2 had stronger connections, and GS3 was similar to HCs except for *Prevotella*. Specific anomalous relationships, such as *Prevotella*–*Streptococcus* (strengthened in GS1, weakened in GS2), were identified. Further details are in Fig. 3c and Supplemental Figures S8–S9.

Clinical and cognitive differences were assessed (Fig. 3d). GSs differed significantly from HCs in MCCB scores ($\eta^2 = 0.614$, $p_{Bonferroni} < 0.001$, 95% *CI* = (197.012, 210.852)) but showed no significant differences in overall PANSS or MCCB scores. However, pairwise comparisons revealed differences in PANSS PScore ($\eta^2 = 0.344$, $p_{Bonferroni} = 0.040$, 95% *CI* = (10.484, 11.842)). Radargram areas for PANSS and MCCB scores also highlighted differences between GSs and HCs, detailed in Supplemental Table S10.

Key biomarkers were identified in association with clinical characteristics. Specifically, in GS1, MCCB scores correlated with *Prevotella*–*Streptococcus* ($r = 0.24$, $p_{Bonferroni}$ = 2.44e-02) and *Bilophila*–*Gemmiger* ($r = 0.24$, $p_{Bonferroni}$ = 2.01e-02). In GS2, PANSS scores correlated with *Ruminococcus*–*Anaerostipes* ($r = 0.52$, $p_{Bonferroni}$ = 3.64e-02), while MCCB scores correlated with *Prevotella*–*Streptococcus* (r = -0.66, $p_{Bonferroni}$ = 4.20e-03). In GS3, *Bifidobacterium*–*Veillonella* was negatively correlated with PANSS TScore (r = -0.35, $p_{Bonferroni}$ = 4.99e-02), and *Prevotella*–*Oscillospira* positively correlated with MCCB visual learning ($r = 0.52$, $p_{Bonferroni}$ = 1.41e-03). See Fig. 3e-g and Supplemental Figure S10 for details.

Two brain–gut subtypes with their corresponding biomarkers

The SC and BIC analysis identified 2 clusters as the optimal number for B-GSs, with an ARI of 0.695. KW tests with Bonferroni correction confirmed no significant differences between training and validation datasets for B-GS1 ($p_{Bonferroni}$ = 0.161) and B-GS2 ($p_{Bonferroni}$ = 0.522). Detailed results are shown in Supplemental Figure S2 and Supplemental Table S8.

Abnormal fusion features differed significantly between the two B-GSs and HCs. In B-GS1, increased features included "ALFF of HES.R–*Oscillospira*" ($\eta^2 = 0.279$, $p_{Bonferroni} < 0.001$, 95% *CI* = (0.123, 0.487)) and "ReHo of CAU.R–*Prevotella*," ($\eta^2 = 0.412$, $p_{Bonferroni} < 0.001$, 95% *CI* = (0.102, 0.358)) while decreased features involved "ReHo of SMG.R–*Oscillospira*" ($\eta^2 = 0.589$, $p_{Bonferroni} < 0.001$, 95% *CI* = (-0.215, -0.104)) and "ReHo of IPL.L–*Oscillospira*." ($\eta^2 = 0.325$, $p_{Bonferroni} < 0.001$, 95% *CI* = (-0.189, -0.105)) For B-GS2, increased features included "ALFF of ORBmid.L–*Oscillospira*" ($\eta^2 = 0.478$, $p_{Bonferroni} < 0.001$, 95% *CI* = (0.547, 0.773)) and "ALFFof FFG.R–*Bacteroides*," ($\eta^2 = 0.529$, $p_{Bonferroni} < 0.001$, 95% *CI* = (0.295, 0.801)) while decreased features involved "WMV of SPG.R–*Veillonella*" ($\eta^2 = 0.298$, $p_{Bonferroni} < 0.001$, 95% *CI* = (-0.654, -0.342)) and "ALFF of PUT.L–*Oscillospira*." ($\eta^2 = 0.364$, $p_{Bonferroni} < 0.001$, 95% *CI* = (-0.614, -0.348)). Fusion features for FC–RA revealed increased SMN–FPN connectivity for B-GS1, while B-GS2 showed strengthened SMN–*Prevotella* connectivity.

Clinical differences between B-GSs and HCs included PANSS PScore ($\eta^2 = 0.430$, $p_{Bonferroni}$ = 0.032, 95% *CI* = (9.546, 12.454)) and significant MCCB differences across dimension ($\eta^2 = 0.458$, $p_{Bonferroni} < 0.001$, 95% *CI* = (203.167, 221.344)). Radargrams highlighted differences in PANSS domains and MCCB scores (Fig. 4b).

Pearson correlations revealed distinct associations. For B-GS1, "ALFF of HES.R–*Oscillospira*" negatively correlated with PANSS PScore (r = -0.40, $p_{Bonferroni}$ = 2.21e-02), and "ReHo of CAU.R–*Prevotella*" correlated with MCCB visual learning (r = -0.40, $p_{Bonferroni}$ = 2.41e-02). For B-GS2, "WMV of SPG.R–*Veillonella*" had a strong negative correlation with PANSS PScore (r = -0.75, $p_{Bonferroni}$ = 9.78e-03), and "GMV of PCG.R–*Oscillospira*" positively correlated with MCCB verbal learning ($r = 0.66$, $p_{Bonferroni}$

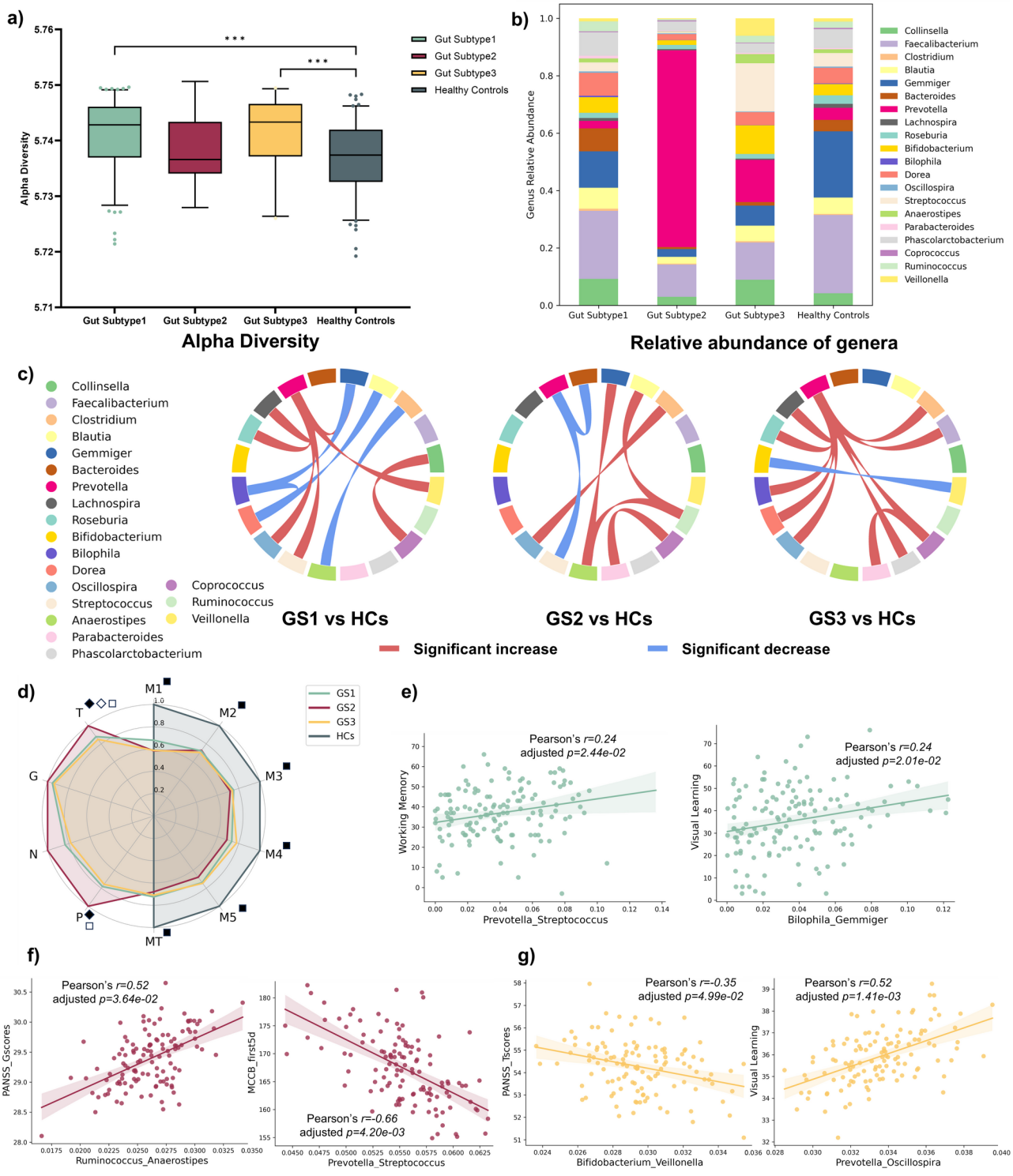

Fig. 3 Differences between the three gut subtypes and their corresponding biomarkers. (**a**) Comparison of alpha diversity between GSs. $^{***}p_{Bonferroni} < 0.001$. (**b**) Differences in RA between GSs. (**c**) Abnormal relationships between genera in GSs compared with HCs. (**d**) Differences in clinical symptoms and cognitive performance vary among GSs and HCs, which are shown as normalized values, where P, N, G, and T represent PANSS PScore, NScore, GScore, and TScore, respectively. M1-M5 and M represent processing speed, attention/vigilance, working memory, verbal learning, visual learning, and total scores of the first five dimensions of the MCCB, respectively. ■$p_{all} < 0.05$, ◆$p_{GSs} < 0.05$, □$p_{GS1\ vs.\ GS2} < 0.05$, and □$p_{GS2\ vs.\ GS3} < 0.05$ (with Bonferroni correction); all values are displayed in Supplemental Table S6. (**e**) Biomarkers of the MCCB score in GS1. (**f**) Biomarkers of the PANSS and MCCB scores in GS2 after bootstrapping. (**g**) Biomarkers of the PANSS and MCCB scores in GS3 after bootstrapping. For the sake of the aesthetics of the graph, the scatter plot was plotted by selecting only the 150 data points obtained after bootstrapping. The error bands in figures (**f-g**) represent 95% confidence interval

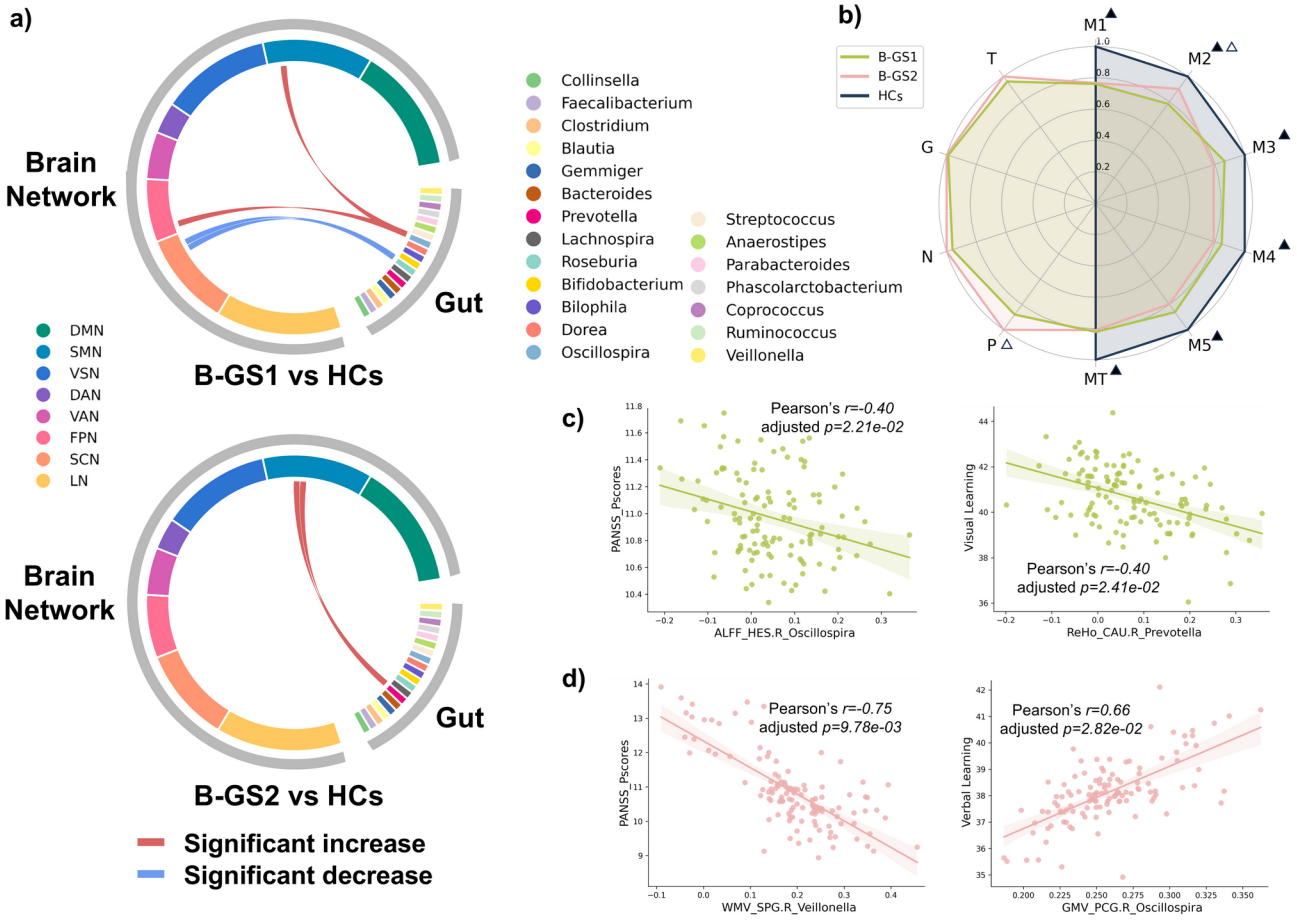

Fig. 4 Differences between the two brain–gut subtypes and their corresponding biomarkers. (**a**) Abnormal FC fusion features of B-GSs and HCs (brain FC from each brain network and RA fusion features for different genera). (**b**) Radar plots show differences in the normalized values of clinical symptoms and cognitive performance for B-GSs and HCs, where P, N, G, and T represent PANSS PScore, NScore, GScore, and TScore, respectively. M1-M5 and M represent processing speed, attention/vigilance, working memory, verbal learning, visual learning, and total scores of the first five dimensions of the MCCB, respectively. ▲$p_{all} < 0.05$ and △$p_{B-GSs} < 0.05$ (with Bonferroni correction), all values are displayed in Supplemental Table S8. (**c**) Biomarkers of the PANSS and MCCB scores in B-GS1 after bootstrapping. (**d**) Biomarkers of the PANSS and MCCB scores in B-GS2 after bootstrapping. For the sake of the aesthetics of the graph, the scatter plot is plotted by selecting only the 150 data points obtained after bootstrapping. The error bands in figures (**c-d**) represent 95% confidence interval

= 2.82e-02). Detailed findings are shown in Fig. 4c-d and Supplemental Figure S14.

Additionally, the mediation analysis results are presented in Supplemental Results S1 and S2. Certain results demonstrate significant mediation effects.

Overlap between the multiple biological subtypes of SZ patients

Among 43 overlapping SZ patients, BS, GS, and B-GS labels were analyzed via Sankey diagrams and scatter plots (Fig. 5, Supplemental Figure S15). B-GS1 and B-GS2 overlapped significantly with BS2. GS1 showed wider distribution across BSs and B-GSs, while GS3 was prevalent in BS2 and B-GS1. Proportions differed notably across subtypes.

Discussion

To the best of our knowledge, this systematic study is the first to analyze the subtypes of SZ by integrating brain imaging, the gut microbiota, and data obtained from their fusion. We applied a data-driven approach and revealed multiple biological subtypes, including two BSs by brain imaging data, three GSs by gut microbiota data, and two B-GSs by brain–gut fusion data, which differed in their typical features and biomarkers. More importantly, the multiple biological subtypes are relatively independent and are related to different clinical symptoms and cognitive performance.

Brain subtypes

In the BS analysis, we identified two subtypes with divergent structural and functional changes. Differences in clinical symptoms and cognitive performance radargrams

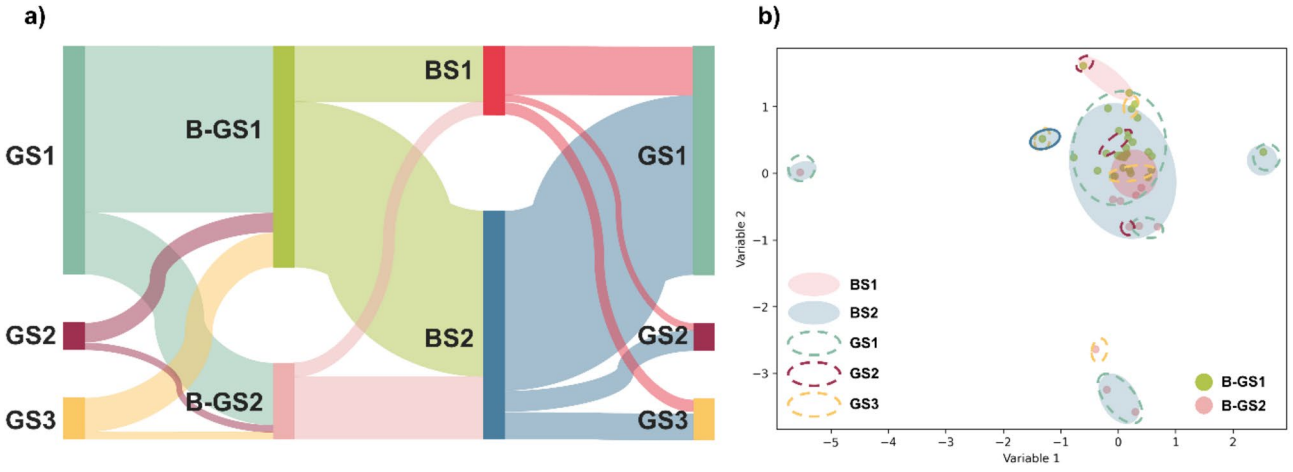

Fig. 5 Overlap between the multiple biological subtypes of SZ. (**a**) Sankey diagram showing the overlap between multiple biological subtypes. (**b**) Scatter plot showing the distribution pattern of subtypes in the three multiple biological datasets

further supported their distinction. These findings align closely with those of previous studies, displaying strong consistency with earlier results [17, 18, 61–64].

BS1 can be described as a structural variant-dominant type with an increased WMV but limited network efficiency and is associated with negative symptoms and cognitive decline. In the analysis of FC and eight networks, we identified localized connectivity abnormalities in the prefrontal lobe of BS1 patients. These abnormalities were predominantly observed within and between networks, particularly in the SMN–LN and intraconnectivity of the VSN. The SMN encompasses functional regions, including the primary motor cortex, cingulate cortex, premotor cortex, and supplementary motor area, as well as the primary somatosensory cortex of the parietal lobe, whereas the VSN is located predominantly within the occipital lobe [53]. Notably, altered WMV in these regions were found to be associated with changes in FC and cognitive performance [65, 66]. This change may impair connectivity between the SMN and the LN and the intraconnectivity of the VSN. These disruptions could significantly diminish the role of BS1 in emotion regulation, memory consolidation, and motor functions, which are largely reliant on sensory and visual processing [67, 68]. Furthermore, diminished SMN connectivity was linked to reduced sensitivity to external stimuli, which may correspond to the higher negative symptom scores observed in the BS1 cohort. This reduced capacity to engage with external stimuli may prompt a heightened focus on internal experiences [69], which in turn correlates with negative symptoms, such as affective flattening.

In contrast, BS2 represents a functional alteration-dominant type with locally reduced WMV but enhanced network efficiency, reflecting more effective communication and information transfer across brain regions, which has been associated with the heightened functional connectivity observed in this group [70, 71]. Additionally, we identified extended connectivity abnormalities in the occipital lobe of BS2 patients, primarily involving internetwork connectivity between the DMN and SMN, VSN, and other networks, as well as intranetwork connectivity within the VAN. Previous studies have linked the DMN and VSN to positive symptoms in SZ patients [72], and our findings corroborate these associations. These findings suggest that this SZ subtype may exhibit increased sensitivity and heightened responses to external stimuli [53, 73]. This increased sensitivity has been correlated with the presence of positive symptoms, including hallucinatory behaviors and heightened agitation, which are commonly observed in SZ patients [18, 62]. Similarly, our analysis of differences in clinical symptoms and cognitive performance further suggested these distinctions, revealing that BS2 exceeded BS1 in working memory, vocabulary learning, and the PANSS PScore. We hypothesized that the elevated connectivity of the DMN–SMN and VSN in BS2 patients may play a role in compensatory effects, relatively offsetting the two cognitive performance scores.

From a clinical perspective, BS1 patients, who exhibit structural abnormalities and negative symptoms, may benefit from neuromodulation such as transcranial magnetic stimulation (TMS) or transcranial direct current stimulation (tDCS) [74], as well as glutamatergic or dopamine-modulating agents to enhance SMN connectivity and alleviate negative symptoms [75]. In contrast, BS2 patients, characterized by hyperconnectivity and positive symptoms, may respond more effectively to dopamine D2 antagonists (e.g., risperidone) [76], and cognitive behavioral therapy for psychosis to help reduce sensory overload [77].

Gut subtypes

Our study further refined previous studies by clustering SZ patients into three subtypes, predominantly dominated by *Collinsella*, *Prevotella*, and *Streptococcus* [29, 34, 78]. Research has shown that *Collinsella* produces the proinflammatory cytokine interleukin-17a and alters gut permeability, which has been associated with systemic inflammation in GS1 patients [79]. This inflammatory response has been linked to gut health issues, which may be related to clinical symptoms. GS3 is characterized by the dominance of *Streptococcus*, which has been shown in previous studies to have neuroactive potential associated with behavioral changes [80]. This microbe has been correlated with abnormal neurobehavioral manifestations in SZ patients. The elevated α diversity in GS1 and GS3 patients indicates a more complex gut microbiota, which may reflect enhanced metabolic redundancy. This increased complexity has been associated with the suppression of inflammatory processes, thereby mitigating clinical symptoms to some extent [81, 82]. Moreover, compared with GS1, GS3 displayed distinct clinical symptom patterns that were likely influenced by the neuroactive properties of *Streptococcus*.

GS2 is dominated by *Prevotella*, which plays a crucial role in the production of short-chain fatty acids (SCFAs) and is associated with weight loss [83]. Interestingly, we observed that GS2 patients had a significantly BMI than did patients with the other subtypes. Previous studies have also indicated an association between BMI and symptom severity [84]. Our findings support this conclusion by suggesting that the link between low BMI and increased symptom severity may be related to the function of *Prevotella*. Previous studies have documented a genetic correlation between SZ and BMI [85]. Our findings provide a novel perspective, indicating that *Prevotella* may be involved in certain underlying biological mechanisms. Additional rigorous investigations are needed to substantiate this hypothesis, and additional research is essential for comprehensive validation. Additionally, the relative abundance of *Prevotella* in GS2 patients was much greater than that reported in previous Western studies, likely because of the traditional diet of the local Han population [83]. Clinically, GS2 patients presented significantly higher positive symptom scores than GS1 and GS3 patients did, suggesting that *Prevotella* may be associated with increase gut permeability, trigger systemic inflammation, and subsequently exacerbate positive symptoms [86]. A recent study reported a bidirectional relationship between inflammation and metabolic function in SZ patients [87]. Taken together, our findings underscore that *Prevotella* could be linked to this relationship. These findings further suggest that interspecies interactions within the gut microbiota can significantly impact physiological and cognitive performance in SZ patients.

From a therapeutic perspective, GS1 patients should receive probiotics (e.g., *Lactobacillus* and *Bifidobacterium*) to reduce inflammation and enhance gut health [38]. GS2 patients may benefit from SCFAs, anti-inflammatory therapies, and weight management to regulate metabolism [38, 83]. GS3 patients should be treated with antipsychotic medications (e.g., olanzapine and risperidone) to modulate the gut microbiota and address behavioral symptoms [88]. Treatment should personalized to microbiota characteristics, focusing on inflammation, metabolism, and neurobehavioral issues.

Brain–gut subtypes

In our study, B-GS1 patients exhibited abnormalities primarily in the functional–genus linkage, where the intersection between brain function and the microbial composition was notably disrupted. Specifically, the weak connectivity observed at the SCN–*Roseburia* intersection aligned with previous studies suggesting a negative correlation between *Roseburia* and functional brain features [41]. This finding suggests that *Roseburia* may be related to variations in the structure and function of the SCN through metabolic pathways, which could be linked to cognitive impairment and mood disturbances in SZ patients, especially reduced attention. This finding reinforces the role of *Roseburia* as a potential factor influencing brain structure via the brain–gut axis.

In contrast, B-GS2 patients displayed structural abnormalities in the brain's linkage to specific gut genera. Abnormal connectivity involving *Oscillospira*, *Lachnospira*, and *Veillonella* was linked to elevated levels of SCFAs and glutamate in the brain, which have been linked to inflammation and neural dysfunction in SZ patients. The associations between these gut microbes and hippocampal glutamate concentrations suggest that *Lachnospira* and *Veillonella* may exacerbate SZ symptoms through excitatory neurotransmitter pathways [89]. These findings underscore the distinct role of B-GS2 in relation to brain structure via interactions with the gut microbiota.

Both B-GS1 and B-GS2 patients exhibited significant connections between the SMN and the gut microbiota, particularly in the "SMN–*Oscillospira*" and "SMN–*Prevotella*" interactions, supporting the mediating role of the SMN in gut–brain communication [40]. In B-GS1 patients, the disrupted *SMN–Roseburia* link was associated with functional alterations, suggesting a differentiated pathway in which these genera are linked to SZ pathophysiology. *Prevotella* was associated with SCFAs production and lipopolysaccharide-binding protein secretion in B-GS2 patients, which have been associated with proinflammatory responses that potentially

influencing brain structures and exacerbate SZ symptoms [83, 90–92]. In addition, BGS2 patients are characterized by heightened attention/vigilance, elevated positive symptom scores, and stronger SMN–*Prevotella* connections. Previous studies have indicated that the SMN, which represents sensorimotor function, has potential as a biomarker for personalized therapy in SZ patients [93]. Furthermore, disruptions in the somatosensory–motor system and inefficient integration of sensory information with attention-demanding processes are significant contributors to SZ-specific cognitive deficits [94]. Our findings expand upon these conclusions by suggesting that the BGS subtype provides a more nuanced characterization of SZ, particularly in relation to sensorimotor and cognitive integration. Both subtypes reveal the critical role of gut–brain interactions in modulating SZ symptoms, providing insights into targeted interventions based on the microbial composition and its impact on brain function.

For personalized treatment of B-GS1 and B-GS2 subtypes, B-GS1 patients may benefit from probiotics (e.g., *Roseburia*) supplemented with prebiotics (e.g., inulin) to restore gut microbiota balance [95], along with an anti-inflammatory Mediterranean diet [96]. Neuromodulation strategies include N-acetylcysteine for glutamate regulation [97], and high frequency TMS or tDCS to enhance SMN function [74]. B-GS2 patients may require SCFAs antagonists, and interleukin-6/tumor necrosis factor-α inhibitors to mitigate inflammation [98], as well as N-Methyl-D-Aspartate receptor modulators (e.g., memantine) to stabilize excitatory neurotransmission [99]. Both subtypes require biomarker monitoring, personalized probiotic interventions, exercise, and stress management for optimal brain-gut regulation.

Comparison of biomarkers of multiple biological subtypes

Each group of the multiple biological subtypes showed significant differences in their respective features, clinical symptoms and cognitive performance, with unique biomarkers. Clinically relevant biomarkers in BS patients were primarily associated with the PANSS score, which revealed more pronounced cognitive differences in BS patients. These findings verify that alterations in brain structure or function significantly impact the cognitive performance of individuals with SZ [100]. Moreover, BSs were validated using public datasets and demonstrated more significantly different features and more robust performance because of the disproportionate differences in sample size [101]. Although the GS patients showed no cognitive differences, their features were significantly correlated with the MCCB scores. The cognitive differences in B-GS patients were not as pronounced as those in BS patients. However, the biomarkers of B-GS patients were associated with both the PANSS and the MCCB scores; in particular, the biomarker of B-GS2 patients had the strongest correlation with clinical symptoms and cognitive performance. The significant correlations between the brain–gut fusion features and the scores of the PANSS or MCCB highlight promising research directions, which may provide more comprehensive insights into the clinical profiles of SZ patients [36, 39]. This approach provides an integrated perspective on both clinical symptoms and cognitive deficits. By integrating brain and gut biomarkers, the analysis of brain–gut fusion improves our understanding of the complex interactions between neurophysiological and microbiome factors, potentially identifying novel therapeutic targets for more personalized and effective interventions in SZ patients.

Limitations

This study has several limitations. Although we identified key interactions between brain and gut features in the study of B-GSs, the small sample size of patients with SZ in the analysis of the brain–gut overlap using the data-driven approach might limit the universality and stability of our findings [101]. Furthermore, the absence of external validation using independent datasets, along with the lack of cross-cohort validation (such as UK Biobank or PNC), may constrain the generalizability of our findings. Additionally, the absence of multicenter study data further limits the generalizability of our findings across different ethnic and geographical contexts.

The lack of follow-up data and medication control also prevented us from analyzing treatment outcomes and the impact of antipsychotic medications on specific subtypes. Although we controlled for potential confounders through inclusion/exclusion criteria, such as medication status, comorbid conditions (e.g., depression, anxiety, metabolic disorders), and lifestyle factors (e.g., diet and exercise habits), the study did not fully account for these influences. Antipsychotic medications are known to significantly alter gut microbiota composition and brain structure, yet we did not perform stratification based on medication use. Additionally, comorbidities that could affect both brain imaging and gut microbiota characteristics were not extensively analyzed. Moreover, lifestyle factors such as diet, which are well-documented to impact gut microbiota composition, were not comprehensively addressed. These limitations may have subtly influenced our results. Furthermore, the cross-sectional design of this study prevents the establishment of causal relationships between brain–gut interactions and clinical symptoms. Future studies should incorporate longitudinal follow-up data to better elucidate the temporal dynamics and causal mechanisms underlying these interactions.

While our findings indicate an association between gut microbiota and brain function, the cross-sectional nature of our study limits causal inferences. Moreover,

we cannot exclude the possibility of reverse causality. Cognitive impairments, schizophrenia symptoms, or medication use may influence gut microbiota composition. Finally, this study did not develop predictive models for patient prognosis or treatment response, which are crucial for translating brain–gut interaction findings into personalized therapeutic strategies. Future research should incorporate machine learning-based predictive modeling to improve clinical applicability.

Conclusions

In conclusion, this study demonstrated that the brain, gut, and their fusion features are heterogeneous among individuals with SZ, whereas the three groups of multiple biological subtypes are independent. The distinct features, clinical symptoms and cognitive performance of patients with different SZ subtypes vary, along with their correlations. These findings show the potential to distinguish SZ subtypes with distinct biomarkers using multiple biological data, thereby suggesting the possibility of personalized and precise treatment for SZ patients.

Abbreviations

SZ	Schizophrenia
sMRI	Structural magnetic resonance imaging
rs-fMRI	Resting-state functional magnetic resonance imaging
WMV	White matter volume
FC	Functional connectivity
HCs	Healthy controls
COBRE	Center for Biomedical Studies Excellence
BMI	Lower body mass index
BSs	Brain subtypes
GSs	Gut subtypes
B-GSs	Brain-gut subtypes
PANSS	Positive and Negative Symptom Scale
MCCB	MATRICS Consensus Cognitive Battery
GMV	Gray matter volume
ALFF	Amplitude of low-frequency fluctuation
ReHo	Regional homogeneity
DMN	Default mode network
SMN	Somatomotor network
VSN	Visual network
DAN	Dorsal attentional network
VAN	Ventral attentional network
FPN	Frontoparietal network
SCN	Subcortical network
LN	Limbic network
RA	Relative abundance
DAE	Denoising autoencoder
ICA	Independent component analysis
GMM	Gaussian mixture mode
SC	Silhouette coefficient
BIC	Bayesian information criterion
ARI	Adjusted rand index
KW	Kruskal–Wallis
η^2	Eta squared
CI	Confidence intervals
SCFAs	Short-chain fatty acids
TMS	Transcranial magnetic stimulation
tDCS	Transcranial direct current stimulation

Supplementary Information

The online version contains supplementary material available at https://doi.org/10.1186/s12967-025-06503-5.

Supplementary Material 1

Acknowledgements

The author extends sincere thanks to the editor and reviewers for their invaluable suggestions and comments, which greatly enhanced the quality of the manuscript. We also wish to express our gratitude to all the volunteers from the Affiliated Brain Hospital, Guangzhou Medical University, and South China University of Technology.

Author contributions

YW: Conceptualization, Data curation, Methodology, Formal analysis, Validation, Visualization, Writing – original draft. SF: Resources, Methodology, Writing – review & editing. YH: Resources, Methodology, Writing – review & editing. RP: Conceptualization, Methodology, Writing – review & editing. LL: Methodology, Writing – review & editing. WW: Writing – review & editing. MG: Writing – review & editing. BZ: Writing – review & editing. HZ: Writing – review & editing. JL: Writing – review & editing. JZ: Methodology, Writing – review & editing. HL: Methodology, Writing – review & editing. XL: Methodology, Writing – review & editing. YN: Methodology, Writing – review & editing. FW: Resources, Supervision, Writing – review & editing. KW: Conceptualization, Funding acquisition, Resources, Supervision, Writing – review & editing. All authors read and approved the final manuscript.

Funding

The funding supported by the National Key Research and Development Program of China (2023YFC2414500, 2023YFC2414504), Natural Science Foundation of China (81971585, 72174082, 82271953 and 82301688), Guangdong Basic and Applied Basic Research Foundation Outstanding Youth Project (2021B1515020064), Key Research and Development Program of Guangdong (2023B0303020001 and 2023B0303010003), Basic and Applied Basic Research Foundation of Guangdong Province (2022A1515140142), Natural Science Foundation of Guangdong Province (2024A1515013058), Science and Technology Program of Guangzhou (202206060005, 202206080005, 202206010077, 202206010034, 202201010093, 2023A03J0856 and 2023A03J0839).

Data availability

The data which has been used in this article is confidential except COBRE.

Declarations

Ethics approval and consent to participate

The study followed the Declaration of Helsinki [44], and was approved by the Ethics Committee of the Affiliated Brain Hospital, Guangzhou Medical University (approval No. (2019)016). Informed consent was obtained from all participants or their legal guardians.

Consent for publication

All participants or their legal guardians provided informed consent for the publication of anonymized data and results derived from this study. No identifiable information is disclosed.

Competing interests

The authors declare that they have no financial conflicts of interest or personal relationships that could have influenced the research presented in this paper.

Author details

[1]School of Biomedical Sciences and Engineering, South China University of Technology, Guangzhou International Campus, Guangzhou 511442, China
[2]Department of Psychiatry, The Affiliated Brain Hospital of Guangzhou Medical University, Guangzhou 510370, China
[3]School of Material Science and Engineering, South China University of Technology, Guangzhou 510006, China

[4]Guangdong Engineering Technology Research Center for Translational Medicine of Mental Disorders, Guangzhou 510370, China
[5]Guangdong Engineering Technology Research Center for Diagnosis and Rehabilitation of Dementia, Guangzhou 510500, China
[6]National Engineering Research Center for Tissue Restoration and Reconstruction, South China University of Technology, Guangzhou 510006, China
[7]Guangdong Province Key Laboratory of Biomedical Engineering, South China University of Technology, Guangzhou 510006, China
[8]Department of Biomedical Engineering, New Jersey Institute of Technology, Newark, NJ, USA
[9]Key Laboratory of Neurogenetics and Channelopathies of Guangdong Province, The Ministry of Education of China, Guangzhou Medical University, Guangzhou 510370, China
[10]Department of Nuclear Medicine and Radiology, Institute of Development, Aging and Cancer, Tohoku University, Sendai 980-8575, Japan

Received: 13 January 2025 / Accepted: 12 April 2025
Published online: 02 May 2025

References

1. Rossler W, Joachim-Salize H, Van Os J, Riecher-Rossler A. Size of burden of schizophrenia and psychotic disorders. Eur Neuropsychopharmacol. 2005;15:399–409.
2. Tost H, Meyer-Lindenberg A. Puzzling over schizophrenia: schizophrenia, social environment and the brain. Nat Med. 2012;18:211–3.
3. Owen MJ, Sawa A, Mortensen PB. Schizophrenia. Lancet. 2016;388:86–97.
4. Howes OD, Onwordi EC. The synaptic hypothesis of schizophrenia version III: a master mechanism. Mol Psychiatry. 2023;28:1843–56.
5. McCutcheon RA, Krystal JH, Howes OD. Dopamine and glutamate in schizophrenia: biology, symptoms and treatment. World Psychiatry. 2020;19:15–33.
6. Kay SR, Fiszbein A, Opler LA. The positive and negative syndrome scale (PANSS) for schizophrenia. Schizophrenia Bull. 1987;13:261–76.
7. Wolfers T, Doan NT, Kaufmann T, Alnæs D, Moberget T, Agartz I, Buitelaar JK, Ueland T, Melle I, Franke B, et al. Mapping the heterogeneous phenotype of schizophrenia and bipolar disorder using normative models. JAMA Psychiatry. 2018;75:1146–55.
8. Fusar-Poli P, Cappucciati M, Borgwardt S, Woods SW, Addington J, Nelson B, Nieman DH, Stahl DR, Rutigliano G, Riecher-Rössler A, et al. Heterogeneity of psychosis risk within individuals at clinical high risk: A Meta-analytical stratification. JAMA Psychiatry. 2016;73:113–20.
9. McCutcheon RA, Pillinger T, Mizuno Y, Montgomery A, Pandian H, Vano L, Marques TR, Howes OD. The efficacy and heterogeneity of antipsychotic response in schizophrenia: A meta-analysis. Mol Psychiatry. 2021;26:1310–20.
10. Brugger SP, Howes OD. Heterogeneity and homogeneity of regional brain structure in schizophrenia: A Meta-analysis. JAMA Psychiatry. 2017;74:1104–11.
11. Jiang Y, Luo C, Wang J, Palaniyappan L, Chang X, Xiang S, Zhang J, Duan M, Huang H, Gaser C, et al. Neurostructural subgroup in 4291 individuals with schizophrenia identified using the subtype and stage inference algorithm. Nat Commun. 2024;15:5996.
12. Lawrie SM, Abukmeil SS. Brain abnormality in schizophrenia: A systematic and quantitative review of volumetric magnetic resonance imaging studies. Br J Psychiatry. 1998;172:110–20.
13. Yu QB, Allen EA, Sui J, Arbabshirani MR, Pearlson G, Calhoun VD. Brain connectivity networks in schizophrenia underlying resting state functional magnetic resonance imaging. Curr Top Med Chem. 2012;12:2415–25.
14. Kha QH, Le VH, Hung TNK, Le NQK. Development and validation of an efficient MRI radiomics signature for improving the predictive performance of 1p/19q Co-Deletion in Lower-Grade gliomas. Cancers (Basel). 2021;13:5398.
15. Le VH, Minh TNT, Kha QH, Le NQK. A transfer learning approach on MRI-based radiomics signature for overall survival prediction of low-grade and high-grade gliomas. Med Biol Eng Comput. 2023;61:2699–712.
16. Dwyer DB, Cabral C, Kambeitz-Ilankovic L, Sanfelici R, Kambeitz J, Calhoun V, Falkai P, Pantelis C, Meisenzahl E, Koutsouleris N. Brain subtyping enhances the neuroanatomical discrimination of schizophrenia. Schizophrenia Bull. 2018;44:1060–9.
17. Chang M, Womer FY, Gong X, Chen X, Tang L, Feng R, Dong S, Duan J, Chen Y, Zhang R, et al. Identifying and validating subtypes within major psychiatric disorders based on frontal-posterior functional imbalance via deep learning. Mol Psychiatry. 2021;26:2991–3002.
18. Chen J, Patil KR, Weis S, Sim K, Nickl-Jockschat T, Zhou J, Aleman A, Sommer IE, Liemburg EJ, Hoffstaedter F, et al. Neurobiological divergence of the positive and negative schizophrenia subtypes identified on a new factor structure of psychopathology using Non-negative factorization: an international machine learning study. Biol Psychiatry. 2020;87:282–93.
19. Liu Z, Palaniyappan L, Wu X, Zhang K, Du J, Zhao Q, Xie C, Tang Y, Su W, Wei Y, et al. Resolving heterogeneity in schizophrenia through a novel systems approach to brain structure: individualized structural covariance network analysis. Mol Psychiatry. 2021;26:7719–31.
20. Liang S, Wang Q, Greenshaw AJ, Li X, Deng W, Ren H, Zhang C, Yu H, Wei W, Zhang Y, et al. Aberrant triple-network connectivity patterns discriminate biotypes of first-episode medication-naive schizophrenia in two large independent cohorts. Neuropsychopharmacology. 2021;46:1502–9.
21. Sun X, Xia M. Schizophrenia and neurodevelopment: insights from connectome perspective. Schizophrenia Bull. 2024;51:309–24.
22. Zhao Y, Zhang Q, Shah C, Li Q, Sweeney JA, Li F, Gong Q. Cortical thickness abnormalities at different stages of the illness course in schizophrenia: A systematic review and Meta-analysis. JAMA Psychiatry. 2022;79:560–70.
23. Jiang Y, Wang J, Zhou E, Palaniyappan L, Luo C, Ji G, Yang J, Wang Y, Zhang Y, Huang C-C, et al. Neuroimaging biomarkers define neurophysiological subtypes with distinct trajectories in schizophrenia. Nat Ment Health. 2023;1:186–99.
24. Xu RH, Wu BB, Liang JW, He FS, Gu W, Li K, Luo Y, Chen JX, Gao YB, Wu Z, et al. Altered gut microbiota and mucosal immunity in patients with schizophrenia. Brain Behav Immun. 2020;85:120–7.
25. Ma X, Asif H, Dai L, He Y, Zheng W, Wang D, Ren H, Tang J, Li C, Jin K, et al. Alteration of the gut Microbiome in first-episode drug-naive and chronic medicated schizophrenia correlate with regional brain volumes. J Psychiatr Res. 2020;123:136–44.
26. Zhu F, Ju Y, Wang W, Wang Q, Guo R, Ma Q, Sun Q, Fan Y, Xie Y, Yang Z, et al. Metagenome-wide association of gut Microbiome features for schizophrenia. Nat Commun. 2020;11:1612.
27. Pan R, Zhang X, Cao J, Yi W, Wei Q, Su H. Analysis of the diversity of intestinal Microbiome and its potential value as a biomarker in patients with schizophrenia: A cohort study. Psychiatry Res. 2020;291:113260.
28. Zhang X, Pan L-y, Zhang Z, Zhou Y-y, Jiang H-y, Ruan B. Analysis of gut mycobiota in first-episode, drug-naïve Chinese patients with schizophrenia: A pilot study. Behav Brain Res. 2020;379:112374.
29. Li Z, Tao X, Wang D, Pu J, Liu Y, Gui S, Zhong X, Yang D, Zhou H, Tao W, et al. Alterations of the gut microbiota in patients with schizophrenia. Front Mol Psychiatry. 2024;15:1366311.
30. Shen Y, Xu J, Li Z, Huang Y, Yuan Y, Wang J, Zhang M, Hu S, Liang Y. Analysis of gut microbiota diversity and auxiliary diagnosis as a biomarker in patients with schizophrenia: A cross-sectional study. Schizophrenia Res. 2018;197:470–7.
31. Yuan X, Zhang P, Wang Y, Liu Y, Li X, Kumar BU, Hei G, Lv L, Huang X-F, Fan X, Song X. Changes in metabolism and microbiota after 24-week Risperidone treatment in drug Naïve, normal weight patients with first episode schizophrenia. Schizophrenia Res. 2018;201:299–306.
32. Gao Y, Liu X, Pan M, Zeng D, Zhou X, Tsunoda M, Zhang Y, Xie X, Wang R, Hu W, et al. Integrated untargeted fecal metabolomics and gut microbiota strategy for screening potential biomarkers associated with schizophrenia. J Psychiatr Res. 2022;156:628–38.
33. Kowalski K, Zebrowska-Rozanska P, Karpinski P, Kujawa D, Laczmanski LL, Samochowiec J, Chic M, Piotrowski P, Misiak B. Profiling gut microbiota signatures associated with the deficit subtype of schizophrenia: findings from a case-control study. Prog Neuro-Psychopharmacol Biol Psychiatry. 2023;127:110834.
34. McGuinness AJ, Davis JA, Dawson SL, Loughman A, Collier F, O'Hely M, Simpson CA, Green J, Marx W, Hair C, et al. A systematic review of gut microbiota composition in observational studies of major depressive disorder, bipolar disorder and schizophrenia. Mol Psychiatry. 2022;27:1920–35.
35. Carabotti M, Scirocco A, Maselli MA, Severi C. The gut-brain axis: interactions between enteric microbiota, central and enteric nervous systems. Ann Gastroenterol. 2015;28:203–9.
36. Cryan JF, O'Riordan KJ, Cowan CSM, Sandhu KV, Bastiaanssen TFS, Boehme M, Codagnone MG, Cussotto S, Fulling C, Golubeva AV, et al. The Microbiota-Gut-Brain Axis. Physiol Rev. 2019;99:1877–2013.
37. Zheng P, Zeng B, Liu M, Chen J, Pan J, Han Y, Liu Y, Cheng K, Zhou C, Wang H, et al. The gut Microbiome from patients with schizophrenia modulates the

glutamate-glutamine-GABA cycle and schizophrenia-relevant behaviors in mice. Sci Adv. 2019;5:eaau8317.
38. Ghaderi A, Banafshe HR, Mirhosseini N, Moradi M, Karimi M-A, Mehrzad F, Bahmani F, Asemi Z. Clinical and metabolic response to vitamin D plus probiotic in schizophrenia patients. BMC Psychiatry. 2019;19:77.
39. Zhu X, Han Y, Du J, Liu R, Jin K, Yi W. Microbiota-gut-brain axis and the central nervous system. Oncotarget. 2017;8:53829–38.
40. Liang L, Li S, Huang Y, Zhou J, Xiong D, Li S, Li H, Zhu B, Li X, Ning Y, et al. Relationships among the gut microbiome, brain networks, and symptom severity in schizophrenia patients: A mediation analysis. Neuroimage Clin. 2024;41:103567.
41. Li S, Song J, Ke P, Kong L, Lei B, Zhou J, Huang Y, Li H, Li G, Chen J, et al. The gut Microbiome is associated with brain structure and function in schizophrenia. Sci Rep. 2021;11:9743.
42. Karakula-Juchnowicz H, Dzikowski M, Pelczarska A, Dzikowska I, Juchnowicz D. The brain-gut axis dysfunctions and hypersensitivity to food antigens in the etiopathogenesis of schizophrenia. Psychiatr Pol. 2016;50:747–60.
43. Wang Y, Wu K. Revealing Multi-biological subtypes of schizophrenia through a Data-Driven clustering. ACM BCB 2024. Volume 73. Shenzhen, China: Association for Computing Machinery; 2024. p. Article73.
44. World Medical A. World medical association declaration of Helsinki: ethical principles for medical research involving human subjects. JAMA. 2013;310:2191–4.
45. Yan C-G, Wang X-D, Zuo X-N, Zang Y-F. DPABI: Data Processing & Analysis for (Resting-State) Brain Imaging. *Neuroinf* 2016, 14:339–351.
46. Kong L-y, Huang Y-y, Lei B-y, Ke P-f, Li H-h, Zhou J, Xiong D-s, Li G-x, Chen J, Li X-b et al. Divergent Alterations of Structural–Functional Connectivity Couplings in First-episode and Chronic Schizophrenia Patients. *Neurosci* 2021, 460:1–12.
47. Chen X, Ke P, Huang Y, Zhou J, Li H, Peng R, Huang J, Liang L, Ma G, Li X, et al. Discriminative analysis of schizophrenia patients using graph convolutional networks: A combined multimodal MRI and connectomics analysis. Front Neurosci. 2023;17:1140801.
48. Chen X, Zhou J, Ke P, Huang J, Xiong D, Huang Y, Ma G, Ning Y, Wu F, Wu K. Classification of schizophrenia patients using a graph convolutional network: A combined functional MRI and connectomics analysis. Biomed Signal Process Control. 2023;80:104293.
49. Guo M, Zhang H, Huang Y, Diao Y, Wang W, Li Z, Feng S, Zhou J, Ning Y, Wu F, Wu K. Transcriptional patterns of nodal entropy abnormalities in major depressive disorder patients with and without suicidal ideation. Research. 2025;8:0659.
50. Andrews-Hanna JR. The brain's default network and its adaptive role in internal mentation. Neuroscientist. 2012;18:251–70.
51. Corbetta M, Shulman GL. Spatial neglect and attention networks. Annu Rev Neurosci. 2011;34:569–99.
52. Uddin LQ, Yeo BTT, Spreng RN. Towards a universal taxonomy of Macro-scale functional human brain networks. Brain Topogr. 2019;32:926–42.
53. Thomas Yeo BT, Krienen FM, Sepulcre J, Sabuncu MR, Lashkari D, Hollinshead M, Roffman JL, Smoller JW, Zöllei L, Polimeni JR, et al. The organization of the human cerebral cortex estimated by intrinsic functional connectivity. J Neurophysiol. 2011;106:1125–65.
54. Tzourio-Mazoyer N, Landeau B, Papathanassiou D, Crivello F, Etard O, Delcroix N, Mazoyer B, Joliot M. Automated anatomical labeling of activations in SPM using a macroscopic anatomical parcellation of the MNI MRI Single-Subject brain. NeuroImage. 2002;15:273–89.
55. Li S, Zhuo M, Huang X, Huang Y, Zhou J, Xiong D, Li J, Liu Y, Pan Z, Li H, et al. Altered gut microbiota associated with symptom severity in schizophrenia. PEERJ. 2020;8:e9574.
56. Li H, Li H, Zhu Z, Xiong X, Huang Y, Feng Y, Li Z, Wu K, Wu F. Association of serum homocysteine levels with intestinal flora and cognitive function in schizophrenia. J Psychiatr Res. 2023;159:258–65.
57. Peng R, Wang W, Liang L, Han R, Li Y, Wang H, Wang Y, Li W, Feng S, Zhou J, et al. The brain-gut microbiota network (BGMN) is correlated with symptom severity and neurocognition in patients with schizophrenia. NeuroImage. 2025;308:121052.
58. Cheng R, Wang L, Le S, Yang Y, Zhao C, Zhang X, Yang X, Xu T, Xu L, Wiklund P, et al. A randomized controlled trial for response of Microbiome network to exercise and diet intervention in patients with nonalcoholic fatty liver disease. Nat Commun. 2022;13:2555.
59. Wang W, Han RJ, Zhang MH, Wang YX, Wang T, Wang YT, Shang XQ, Peng JJ. A network-based method for brain disease gene prediction by integrating brain connectome and molecular network. Briefings Bioinf. 2022;23:bbab459.
60. Shrout PE, Bolger N. Mediation in experimental and nonexperimental studies: new procedures and recommendations. Psychol Methods. 2002;7:422–45.
61. Tijms BM, Vromen EM, Mjaavatten O, Holstege H, Reus LM, van der Lee S, Wesenhagen KEJ, Lorenzini L, Vermunt L, Venkatraghavan V, et al. Cerebrospinal fluid proteomics in patients with Alzheimer's disease reveals five molecular subtypes with distinct genetic risk profiles. Nat Aging. 2024;4:33–47.
62. Chand GB, Dwyer DB, Erus G, Sotiras A, Varol E, Srinivasan D, Doshi J, Pomponio R, Pigoni A, Dazzan P, et al. Two distinc neuroanatomica subtypes of schizophrenia revealed using machine learning. Brain. 2020;143:1027–38.
63. Chai C, Ding H, Du X, Xie Y, Man W, Zhang Y, Ji Y, Liang M, Zhang B, Ning Y, et al. Dissociation between neuroanatomical and symptomatic subtypes in schizophrenia. Eur Psychiatry. 2023;66:e78.
64. Okada N, Fukunaga M, Miura K, Nemoto K, Matsumoto J, Hashimoto N, Kiyota M, Morita K, Koshiyama D, Ohi K, et al. Subcortical volumetric alterations in four major psychiatric disorders: a mega-analysis study of 5604 subjects and a volumetric data-driven approach for classification. Mol Psychiatry. 2023;28:5206–16.
65. Filley CM, Fields RD. White matter and cognition: making the connection. J Neurophysiol. 2016;116:2093–104.
66. Gao Y, Li M, Huang AS, Anderson AW, Ding Z, Heckers SH, Woodward ND, Gore JC. Lower functional connectivity of white matter during rest and working memory tasks is associated with cognitive impairments in schizophrenia. Schizophrenia Res. 2021;233:101–10.
67. Buchsbaum BR, D'Esposito M. A sensorimotor view of verbal working memory. Cortex. 2019;112:134–48.
68. Tranfa M, Iasevoli F, Cocozza S, Ciccarelli M, Barone A, Brunetti A, de Bartolomeis A, Pontillo G. Neural substrates of verbal memory impairment in schizophrenia: A multimodal connectomics study. Hum Brain Mapp. 2023;44:2829–40.
69. Strauss GP, Llerena K, Gold JM. Attentional disengagement from emotional stimuli in schizophrenia. Schizophrenia Res. 2011;131:219–23.
70. Fernandez-Linsenbarth I, Planchuelo-Gomez A, Beno-Ruiz-de-la-Sierra RM, Diez A, Arjona A, Perez A, Rodriguez-Lorenzana A, del Valle P, Luis-Garcia R, Masciliano G, et al. Search for schizophrenia and bipolar biotypes using functional network properties. Brain Behav. 2021;11:e2415.
71. Yu M, Dai Z, Tang X, Wang X, Zhang X, Sha W, Yao S, Shu N, Wang X, Yang J, et al. Convergence and divergence of brain network dysfunction in deficit and Non-deficit schizophrenia. Schizophrenia Bull. 2017;43:1315–28.
72. Hu ML, Zong XF, Mann JJ, Zheng JJ, Liao YH, Li ZC, He Y, Chen XG, Tang JS. A review of the functional and anatomical default mode network in schizophrenia. Neurosci Bull. 2017;33:73–84.
73. Androulakis XM, Krebs KA, Jenkins C, Maleki N, Finkel AG, Rorden C, Newman R. Central executive and default mode network intranet work functional connectivity patterns in chronic migraine. J Neurol Disord. 2018;6:393.
74. Zhou Y, Xia X, Zhao X, Yang R, Wu Y, Liu J, Lyu X, Li Z, Zhang G, Du X. Efficacy and safety of transcranial direct current stimulation (tDCS) on cognitive function in chronic schizophrenia with tardive dyskinesia (TD): a randomized, double-blind, sham-controlled, clinical trial. BMC Psychiatry. 2023;23:623.
75. Krogmann A, Peters L, von Hardenberg L, Bödeker K, Nöles VB, Correill CU. Keeping up with the therapeutic advances in schizophrenia: a review of novel and emerging Pharmacological entities. CNS Spectr. 2019;24:41–68.
76. He H, Richardson JS. A Pharmacological, Pharmacokinetic and clinical overview of Risperidone, a new antipsychotic that blocks serotonin 5-HT2 and dopamine D2 receptors. Int Clin Psychopharm. 1995;10:19–30.
77. Yuan S, Wu H, Wu Y, Xu H, Yu J, Zhong Y, Zhang N, Li J, Xu Q, Wang C. Neural effects of cognitive behavioral therapy in psychiatric disorders: A systematic review and activation likelihood Estimation Meta-Analysis. Front Psychol. 2022;13:853804.
78. Nikolova VL, Smith MRB, Hall LJ, Cleare AJ, Stone JM, Young AH. Perturbations in gut microbiota composition in psychiatric disorders: A review and Meta-analysis. JAMA Psychiatry. 2021;78:1343–54.
79. Chen J, Wright K, Davis JM, Jeraldo P, Marietta EV, Murray J, Nelson H, Matteson EL, Taneja V. An expansion of rare lineage intestinal microbes characterizes rheumatoid arthritis. Genome Med. 2016;8:43.
80. Valles-Colomer M, Falony G, Darzi Y, Tigchelaar EF, Wang J, Tito RY, Schiweck C, Kurilshikov A, Joossens M, Wijmenga C, et al. The neuroactive potential of the human gut microbiota in quality of life and depression. Nat Microbiol. 2019;4:623–32.
81. Larsen OFA, Claassen E. The mechanistic link between health and gut microbiota diversity. Sci Rep. 2018;8:2183.
82. Lozupone CA, Stombaugh JI, Gordon JI, Jansson JK, Knight R. Diversity, stability and resilience of the human gut microbiota. Nat. 2012;489:220–30.

83. Tett A, Pasolli E, Masetti G, Ercolini D, Segata N. Prevotella diversity, niches and interactions with the human host. Nat Rev Microbiol. 2021;19:585–99.
84. Sun XB, He RQ, Xiao Y, Xiu MH, Sun MD, Wu FC, Zhang XY. Interaction between baseline BMI and baseline disease severity predicts greater improvement in negative symptoms in first-episode schizophrenia. Eur Arch Psychiatry Clin Neurosci. 2024;274:1327–32.
85. Yu YF, Fu YQ, Yu YT, Tang MJ, Sun Y, Wang YY, Zhang K, Li HX, Guo H, Wang B, et al. Investigating the shared genetic architecture between schizophrenia and body mass index. Mol Psychiatry. 2023;28:2312–9.
86. Doorduin J, de Vries EFJ, Willemsen ATM, de Groot JC, Dierckx RA, Klein HC. Neuroinflammation in Schizophrenia-Related psychosis: A PET study. J Nucl Med. 2009;50:1801–7.
87. Van Dyne A, Wu TC, Adamowicz DH, Lee EE, Tu XM, Eyler LT. Longitudinal relationships between BMI and hs-CRP among people with schizophrenia. Schizophrenia Res. 2024;271:337–44.
88. Dinarello CA. Anti-inflammatory agents: present and future. Cell. 2010;140:935–50.
89. Joe P, Clemente JC, Piras E, Wallach DS, Papp JR, Boka E, Remsen B, Bonner M, Kimhy D, Goetz D, et al. An integrative study of the Microbiome gut-brain-axis and hippocampal inflammation in psychosis: persistent effects from mode of birth. Schizophrenia Res. 2022;247:101–15.
90. Scheurink TAW, Borkent J, Gangadin SS, El Aidy S, Mandl R, Sommer IEC. Association between gut permeability, brain volume, and cognition in healthy participants and patients with schizophrenia spectrum disorder. Brain Behav. 2023;13:e3011.
91. Gokulakrishnan K, Nikhil J, Vs S, Holla B, Thirumoorthy C, Sandhya N, Nichenametla S, Pathak H, Shivakumar V, Debnath M, et al. Altered intestinal permeability biomarkers in schizophrenia: A possible link with subclinical inflammation. Ann Neurosci. 2022;29:151–8.
92. Park BS, Lee J-O. Recognition of lipopolysaccharide pattern by TLR4 complexes. Exp Mol Med. 2013;45:e66.
93. Hirjak D, Meyer-Lindenberg A, Sambataro F, Fritze S, Kukovic J, Kubera KM, Wolf RC. Progress in sensorimotor neuroscience of schizophrenia spectrum disorders: lessons learned and future directions. Prog Neuro-Psychopharmacol Biol Psychiatry. 2021;111:110370–110370.
94. Dong DB, Yao DZ, Wang YL, Hong SJ, Genon S, Xin F, Jung K, He H, Chang XB, Duan MJ, et al. Compressed sensorimotor-to-transmodal hierarchical organization in schizophrenia. Psychol Med. 2023;53:771–84.
95. Wang S, Xiao Y, Tian F, Zhao J, Zhang H, Zhai Q, Chen W. Rational use of prebiotics for gut microbiota alterations: specific bacterial phylotypes and related mechanisms. J Funct Foods. 2020;66:103838.
96. Itsiopoulos C, Mayr HL, Thomas CJ. The anti-inflammatory effects of a mediterranean diet: a review. Curr Opin Clin Nutr Metab Care. 2022;25:415–22.
97. Yang YS, Maddock RJ, Zhang H, Lee J, Hellemann G, Marder SR, Green MF. N-Acetylcysteine effects on glutathione and glutamate in schizophrenia: A preliminary MRS study. Psychiatry Res Neuroimaging. 2022;325:111515.
98. Li M, van Esch BCAM, Wagenaar GTM, Garssen J, Folkerts G, Henricks PAJ. Pro- and anti-inflammatory effects of short chain fatty acids on immune and endothelial cells. Eur J Pharmacol. 2018;831:52–9.
99. Kikuchi T. Is memantine effective as an NMDA receptor antagonist in adjunctive therapy for schizophrenia?? Biomolecules. 2020;10:1134.
100. Geisler D, Walton E, Naylor M, Roessner V, Lim KO, Charles Schulz S, Gollub RL, Calhoun VD, Sponheim SR, Ehrlich S. Brain structure and function correlates of cognitive subtypes in schizophrenia. Psychiatry Res. 2015;234:74–83.
101. Yarkoni T. Big correlations in little studies: inflated fMRI correlations reflect low statistical power. Perspect Psychol Sci. 2009;4:294–8.

Publisher's note